**Ninth Canadian Conference on
Earthquake Engineering
Ottawa, Ontario, Canada
26-29 June 2007**

# BEHAVIOUR OF CONCRETE COLUMNS WITH FRP SHELLS AS CONFINEMENT REINFORCEMENT

S. A. Sheikh[1] and C. Cui[2]

## ABSTRACT

The paper presents the results of an experimental program on the behavior of concrete filled Fiber reinforced polymer (FRP) shells subjected to axial load. Columns, 356mm in diameter and 1524mm in height, were tested under axial compression. Variables involved were type of FRP, number of FRP layers and their orientation, and the amount of longitudinal and lateral steel. The test results demonstrate that FRP shells can be effectively used as stay-in-place formwork and confinement reinforcement thus improving the seismic resistance of columns significantly by enhancing their strength, ductility and energy absorption capacity. In addition, 152mm by 305mm cylinders wrapped with same CFRP and GFRP were tested to identify the size effect on the behavior of confined concrete. It is concluded that larger size columns achieved more desirable performance by failing in a relatively ductile manner.

## Introduction

Reinforced concrete has been used successfully for decades. However, environmental effects such as freeze-thaw cycles, low temperatures, UV radiation, and chlorides from salts significantly affect long term performance of concrete structures. For instance, inevitable damage from corrosion of the steel can lead to the cracking, spalling, and delamination of concrete as well as the loss of reinforcing steel cross section, and as a consequence, reduce the load carrying capacity of the reinforced concrete members. Brittle failure of the columns can result in the collapse of the entire structure, particularly during severe earthquakes. FRP jackets have been increasingly popular in repair and strengthening of concrete columns, due to their light weight, high strength, flexibility in shape and size, durability, and savings on labor cost and construction time. Based on the experimental and corresponding analytical work in the literature, columns retrofitted with FRP wraps have demonstrated remarkably enhanced performance including improvements in strength, ductility, and energy absorption capacity.

Concrete structures with traditional reinforcements are susceptible to deterioration that requires considerable rehabilitation during their lifespan. To minimize these costly operations and increase the durability of newly constructed infrastructure, one can envision casting concrete in a permanent formwork that is prefabricated from FRP composites. This study was aimed at examining the use of FRP shells as stay-in-place forms and confining reinforcement for concrete columns. Also, a comparative study of concrete columns confined with FRP shell and concrete cylinders wrapped with FRP jackets was carried out to investigate the size effect on the effectiveness of FRP confinement.

[1]Professor, Dept. of Civil Engineering, University of Toronto, Toronto, ON, M5S 1A4
[2]Graduate Research Assistant, Dept. of Civil Engineering, University of Toronto, Toronto, ON, M5S 1A4

## Experimental Work

### Specimens

Large scale circular columns, 356mm in diameter and 1524mm in height, were constructed and tested under concentric compression (Cairns and Sheikh 2001, Jaffry and Sheikh 2001). Specimens can be divided into three groups: 6 control specimens without FRP jackets, 11 each constructed with carbon FRP and glass FRP shells. In each group, there are three types of specimens based on the steel reinforcement used: specimens with no longitudinal or lateral steel, specimens with longitudinal steel and steel hoops at 320 mm spacing, and specimens with longitudinal steel and steel spirals at 75 mm pitch. Other variables included number of layers of FRP and orientation of fibers in the FRP shells. In addition, more than one hundred cylinders (152 x 305 mm), mostly confined with FRP, were tested. Results from eight cylinder tests are discussed in this paper to evaluate the size effect. Details of these cylinder specimens are provided under Results and in Table 2.

Table 1. Details of columns and test results.

| Spec. No. | Name | Lateral steel Size (US#) | Lateral steel Spacing (mm) | Longitudinal steel No. of bars | Longitudinal steel Size (#) | FRP layers | $f_{ccmax}$ (MPa) | $\varepsilon_{cc}'$ * | k $=f_{ccmax}/0.85f_c'$ | μ | $e_{80}$ | $e_{50}$ | $e_{20}$ | W80 | W50 | W20 |
|---|---|---|---|---|---|---|---|---|---|---|---|---|---|---|---|---|
| 1 | 00-10-1 | - | - | 1 | 20M | 0 | 30.70 | 0.00140 | 1.20 | 3.19 | 0.081 | NA | NA | 2.520 | NA | NA |
| 3 | 00-LS320-3 | #3 | 320 | 6 | 20M | 0 | 25.86 | 0.00170 | 1.01 | 4.92 | 0.092 | 0.122 | 0.153 | 4.020 | 5.350 | 6.700 |
| 4 | 00-LS320-4 | #3 | 320 | 6 | 20M | 0 | 30.08 | 0.00211 | 1.18 | NA | NA | NA | NA | NA | NA | NA |
| 5 | 00-LS75-5 | #3 | 75 | 6 | 20M | 0 | 44.00 | 0.00400 | 1.73 | 9.27 | 0.513 | 0.936 | NA | 7.750 | 14.150 | NA |
| 6 | 00-LS75-6 | #3 | 75 | 6 | 20M | 0 | 44.00 | 0.00462 | 1.73 | 10.26 | 0.584 | 0.900 | 1.120 | 8.840 | 13.620 | 16.950 |
| 7 | G01-00-7 | - | - | - | - | 1GFRP | 34.77 | 0.00370 | 1.36 | 9.08 | 0.336 | 0.517 | 0.660 | 8.140 | 12.530 | 16.000 |
| 8 | G11-00-8 | - | - | - | - | 2GFRP$ | 38.41 | 0.00403 | 1.51 | 8.57 | 0.390 | 0.500 | 0.830 | 7.750 | 9.930 | 16.480 |
| 9 | G01-L0-9 | - | - | 6 | 20M | 1GFRP | 32.43 | 0.00739 | 1.27 | 10.81 | 0.350 | 0.490 | NA | 9.750 | 13.650 | NA |
| 10 | G01-LS320-10 | #3 | 320 | 6 | 20M | 1GFRP | 37.19 | 0.01151 | 1.46 | 14.30 | 0.580 | 0.680 | 0.800 | 12.290 | 14.410 | 16.950 |
| 11 | G02-00-11 | - | - | - | - | 2GFEP | 44.82 | 0.01199 | 1.76 | 13.56 | 0.817 | 1.186 | 1.346 | 11.920 | 17.300 | 19.630 |
| 12 | G22-00-12 | - | - | - | - | 4GFRP# | 54.76 | 0.00979 | 2.15 | 14.16 | 1.320 | 1.528 | 1.716 | 12.900 | 14.930 | 16.770 |
| 14 | G02-LS320-14 | #3 | 320 | 6 | 20M | 2GFRP | 49.31 | 0.01792 | 1.93 | 15.49 | 1.070 | 1.570 | 1.690 | 12.890 | 18.920 | 20.360 |
| 15 | G02-LS75-15 | #3 | 75 | 6 | 20M | 2GFRP | 54.00 | 0.01672 | 2.12 | 16.49 | 1.420 | 2.100 | NA | 14.270 | 21.100 | NA |
| 19 | C11-00-19 | - | - | - | - | 2CFRP$ | 48.40 | 0.01108 | 1.73 | 13.30 | 0.955 | 1.012 | 1.063 | 12.220 | 12.950 | 13.6 |
| 20 | C01-L0-20 | - | - | 6 | 20M | 1CFRP | 43.90 | 0.00888 | 1.56 | 14.70 | 0.835 | 0.940 | 0.97 | 13.000 | 14.640 | 15.1 |
| 21 | C01-LS320-21 | #3 | 320 | 6 | 20M | 1CFRP | 43.40 | 0.00944 | 1.60 | 17.70 | 0.964 | 1.059 | 1.073 | 15.380 | 16.890 | 17.110 |
| 24 | C02-00-24 | - | - | - | - | 2CFRP | 59.30 | 0.01375 | 2.11 | 16.10 | 1.654 | 1.782 | 1.839 | 14.130 | 15.220 | 15.71 |
| 25 | C22-00-25 | - | - | - | - | 4CFRP# | 58.30 | 0.01097 | 2.06 | 13.20 | 1.365 | 1.459 | 1.499 | 12.040 | 12.870 | 13.23 |
| 27 | C02-LS320-27 | #3 | 320 | 6 | 20M | 2CFRP | 57.00 | 0.01442 | 2.01 | 14.40 | 1.338 | 1.464 | NA | 12.370 | 13.530 | NA |
| 28 | C02-LS75-28 | #3 | 75 | 6 | 20M | 2CFRP | 66.60 | 0.01884 | 2.35 | 13.30 | 1.645 | 1.792 | 2.056 | 11.130 | 12.120 | 13.91 |

$ One layer of FRP in the longitudinal direction and one in lateral direction

# Two layers of FRP in the longitudinal direction and two in lateral direction

* Axial strain corresponding to the $f_{ccmax}$

The details for the columns considered in this study are displayed in Table 1. The alphanumeric name of each column explains the information of its configuration. The first letter “G” or “C” represents the presence of GFRP or CFRP shell and it is omitted for group one specimens without FRP shells. The digit following the first letter indicates the number of layers of FRP in the longitudinal direction, and the next digit indicates the number of layers of FRP in the lateral direction. The letter “L” or digit “0” after the numbers reveals the presence or non-existence, respectively, of 6 longitudinal 20M steel bars. The next digit “0” or letter “S” followed by a number “75” or letter “S” followed by a number “320” indicates no lateral steel, US #3 lateral hoops at 320mm spacing, or US #3 spirals at 75mm pitch, respectively. Finally, the last number indicates the specimen number. Hence, for instance, specimen C02-LS75-28 has no carbon fiber in longitudinal direction, 2 layer of carbon fiber in lateral direction, longitudinal reinforcement with lateral steel spaced at 75 mm, and the specimen number of 28. Specimens 1 and 2 were made of plain concrete without any GFRP shells and contained only one longitudinal bar in the centre for the purpose of handling the specimen safely before and after testing. In the designation of these two specimens, the number ‘1’ instead of letter “L” denotes only one longitudinal bar in the specimen.

***Concrete:*** A ready-mixed concrete with a slump of around 150mm was used. Nineteen 150 × 300 mm concrete cylinders were cast with the columns and tested at various ages after casting to track the strength development of concrete. According to ASTM Standard C39/C39M-00, the 28-day concrete cylinder strength ranged between 29.0 MPa and 30.3 MPa with an average of 29.8 MPa and the corresponding longitudinal compressive strain at peak stress varied between 0.0018 and 0.0019.

***Steel:*** Grade 400, 20M bars (cross sectional area of 300 $mm^2$) were used as longitudinal steel and Grade 60 US #3 bars (cross sectional area of 71 $mm^2$) were used for lateral reinforcement. Based on ASTM A370-00, the yield stresses for these two bars were 402 MPa and 500 MPa, respectively, with corresponding yield strains of 0.002102 and 0.00255. Clear concrete cover in the columns was 20 mm to the lateral steel and about 30 mm to the longitudinal steel.

***Fiber reinforced polymers (FRP):*** Prefabricated shells with inner diameter of 356mm were manufactured with varying volume and configuration/orientation of fibers. According to ASTM D3039-00, eight coupons of each FRP material were tested for tensile properties along the fibers. The average tensile strength was 535 and 885 N/mm width and the average rupture strain was 0.0237 and 0.0125 for one layer of 1mm thick GFRP and 0.5mm thick CFRP, respectively.

**Construction and testing of specimens**

***Construction:*** Cylindrical sonotubes and prefabricated FRP shells were utilized as formworks for control specimens and FRP confined specimens, respectively. Three different steel cages with various steel arrangements were built and used in columns as shown in Table 1. Each specimen had four threaded rods placed through to mount external Linear Variable Differential Transducers (LVDTs) to measure longitudinal deformation of the column. Concrete was placed in three layers for each specimen, with each layer carefully vibrated using a hand held concrete vibrator. Wet burlap and plastic sheeting were placed over the specimens for a three-day curing. After that, plastic and burlap were removed for air cure. The specimens stayed within the formwork until concrete strength of 20 MPa was obtained from the cylinder tests. Extra layers of GFRP were applied in the end regions of each column to prevent premature failure outside the test region.

***Instrumentation:*** LVDTs or strain gauges were used to measure longitudinal column deformations, longitudinal steel bar strains, longitudinal GFRP strains, lateral steel strains, and lateral GFRP strains. Four LVDTs were mounted 90° apart to the embedded rods to measure the longitudinal deformation of columns. Strain gauges were applied to longitudinal bars and lateral steels. One strain gauge was attached to each longitudinal bar at the mid-height of the column. The spirals with 75 mm pitch had four gauges at 90° from each other in the middle of the test region. The specimens containing hoops at 320 mm had two hoops in the test region instrumented with 4 strain gauges each at 90° apart. Strain gauges were also installed at the column mid-height of the shell surface. Two gauges were aligned longitudinally and two laterally, with gauges of the same orientation located on opposite sides of each column.

***Testing:*** A steel frame, with 8900-kN capacity, was used to test the specimens. Plaster was applied at top and bottom to ensure smooth and even transfer of the axial load. After all the LVDTs were attached, the specimen was loaded to around 20% of its expected loading capacity. In case the comparable readings were found to differ by more than 5%, the specimen was un-loaded, adjusted, and then re-loaded till reasonable alignment was obtained. Each specimen was subjected to monotonically increasing axial load until complete failure of the specimen was achieved. Load was applied at an average rate of approximately 100 kN/sec or 1 MPa/sec over the gross column area, with the highest average rate of 180 kN/sec. Data from LVDTs and the load cell were recorded by a computer-controlled data acquisition system configured to read one hundred sets of readings per second.

## Results

### Test observations

Control specimens 1 and 2 failed in a brittle fashion with deep "popping" sounds as a sudden burst of concrete occurred in the test region. Control columns 3 and 4, both with steel hoops at 320mm spacing, failed in a relatively quite manner: the concrete cover spalled off immediately followed by an outburst of the core concrete and buckling of the longitudinal bars. Control specimens 5 and 6 failed in a more ductile manner due to considerable confinement of the core concrete provided by #3 spirals at 75mm pitch. As the column strain exceeded around 0.0018, the crushing strain for plain concrete cylinder test, the concrete cover experienced severe damage. Owe to the spiral confinement, core concrete could carry the increasing load while expansion of core concrete carried on. At a later stage, the longitudinal bars started bucking and concrete core expanded pushing out the lateral spiral and causing rupture of spirals at several locations. Eventually, concrete columns failed with the crushing of concrete.

All the specimens confined with FRP shells failed in the test region except for specimen 18, which will be excluded in the following discussion. In addition, specimens 13 failed under eccentric load although great efforts were made to avoid this type of failure. Thus specimen 13 is also not considered in the analysis.

Other than specimens 13 and 18, all the columns containing FRP in the circumferential direction failed in a similar manner. The failure was initiated by the rupture of FRP in the test region. The rupture of GFRP shell was found starting at one location and, with a sudden burst, moved around in the circumferential direction rapidly. When the CFRP shell ruptured vertically at certain load they peeled away from the concrete core by tearing horizontally.

### Column performances

Stress-strain curves of confined concrete, which significantly characterize performance of columns, can be obtained from the test data. As illustrated in Fig. 1a, the contribution of the concrete in carrying the load was determined by subtracting the contribution of longitudinal bars, if there are any, from the total applied load at a particular strain level. For specimens with fibers partially oriented in the longitudinal direction, the contribution from longitudinal FRP was ignored. The gross concrete cross-sectional area was used to obtain the concrete stress for FRP confined specimens and control specimens 1, 2, 3 and 4 which contained little or no confinement. Core concrete in specimens 5 and 6 is effectively confined with spiral at 75mm pitch, thus the core and the cover concretes behaved differently. It was suggested by Sheikh and Uzumeri (1980) that the cover starts spalling off at a strain corresponding to the plain concrete strength and becomes completely ineffective at a strain corresponding to 50% of the peak stress of plain concrete on the descending branch of its stress-strain curve. Assuming a linear variation of effective concrete area from the total concrete area to the core concrete area between these two strain values, the confined concrete stress strain response can be determined as shown in Fig. 1b.

Stress-strain responses of specimens with FRP shells mostly consisted of two ascending branches before peak stress followed by a post-peak descending branch. The slope of the first branch was almost the same as that of unconfined concrete specimens. The second branch was less steep in slope and more distinctly linear for the specimens with higher lateral confinement. The slope of the descending branch depends on the properties of confining materials among other factors. From the stress-strain curves of specimens, strength enhancement, ductility, energy absorption capacity, and work indices were computed to evaluate the performance of columns.

***Strength enhancement factor k:*** Strength enhancement with respect to column concrete strength was calculated using Eq. 1 (Sheikh and Uzumeri 1980):

$$k = f_{ccmax}/0.85f_c' \qquad (1)$$

where $f_{ccmax}$ is confined concrete strength and $f_c'$ is unconfined concrete strength obtained from standard cylinder tests.

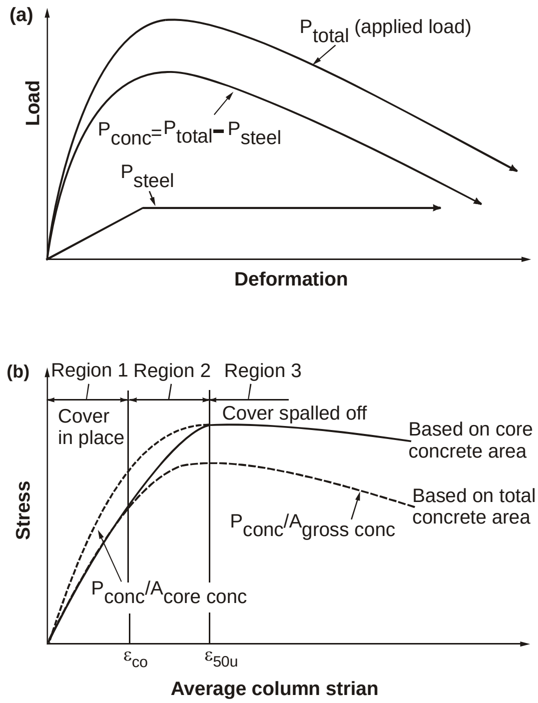


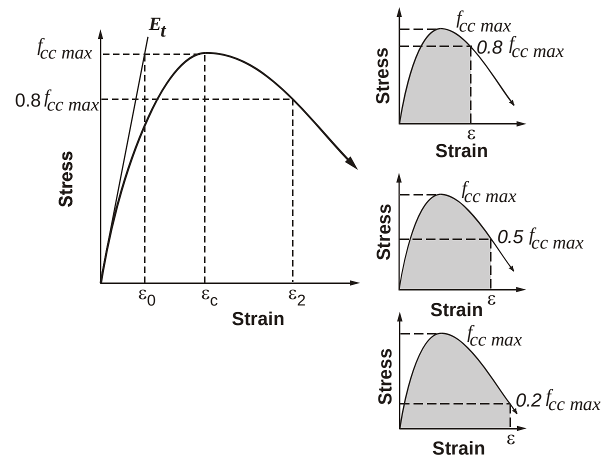


Figure1. Concrete contribution curves.

Figure 2. Typical confined concrete stress-strain curve.

***Ductility factor $\mu$:*** The ductility factor, calculated from Eq. 2, was used to evaluate deformation ability of columns without significant strength loss (Fig. 2):

$$\mu=\varepsilon_2/\varepsilon_0 \qquad (2)$$

where $\varepsilon_0$ is the axial strain corresponding to the maximum confined concrete stress ($f_{ccmax}$) on the initial tangent $E_t$ and $\varepsilon_2$ is the axial strain corresponding to a strength of $0.8f_{ccmax}$ on the descending portion of the stress-strain curve.

***Energy absorption capacity $e_i$:*** The energy absorption capacity ($e_i$) indicates the amount of energy absorbed by specimens. It is defined as the area under the stress-strain curve of confined concrete up to a certain level of stress. In this study, three levels of stress were adopted for the energy absorption calculation: 80%, 50% and 20% of peak strength $f_{ccmax}$ on the descending branch of the curve. The corresponding energy absorption capacities were denoted as $e_{80}$, $e_{50}$, and $e_{20}$ (Fig. 2), respectively.

***Work Index $W_i$* :** The energy capacity calculated was normalized to obtain a dimensionless parameter termed as Work Index ($W_i$) (Eq.3).

$$W_i= e_i /(f_{ccmax} \times \varepsilon_0) \qquad (3)$$

**Effects of different variables**

***Effect of lateral FRP on column behavior:*** FRP jackets with fibers in the lateral direction have been reported to significantly improve column behaviors including strength and ductility. In this study, the improvement from FRP shells can be observed from three groups of specimens: columns 1, 7, 11, 20, and 24, with neither longitudinal bars nor lateral steel (Fig. 3a); columns 3, 10, 14, 21 and 27, with six longitudinal bars and lateral hoops at 320mm spacing (Fig. 3b); and columns 6, 15, and 28, with longitudinal bars and spirals at 75mm pitch (Fig. 3c). First specimen in each group was the control specimen without FRP confinement. The rest of specimens in each group were specimens with GFRP or CFRP shells. As can be observed from Fig. 3 and Table 1, the strength, ductility, and energy absorption capacity of columns significantly increased due to the presence of FRP. The improvement increased with an increase in the number of FRP layers.

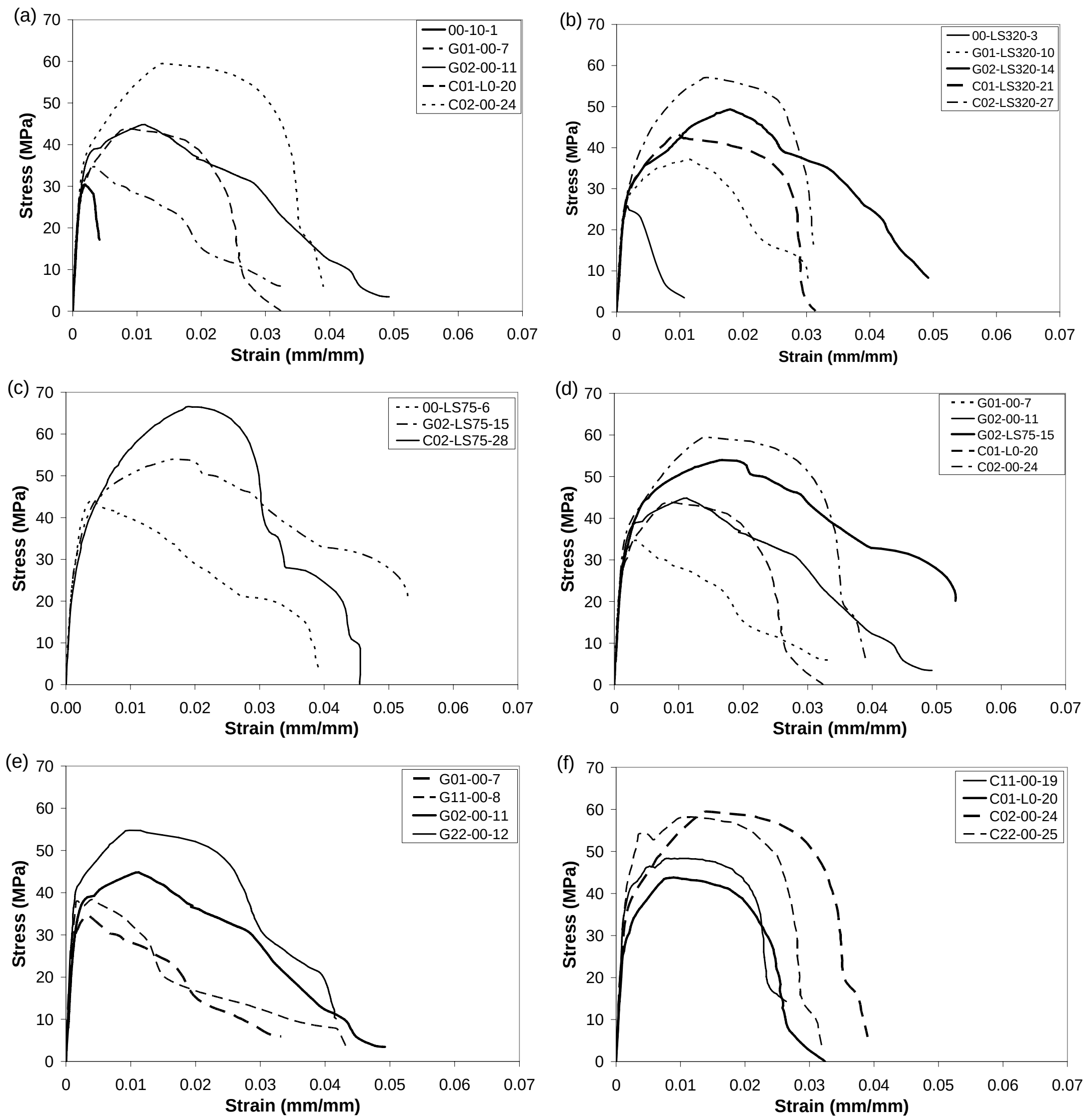


Figure 3. Comparison between axial stress-axial strain of specimens: (a) specimens with no lateral steel; (b) specimens with steel hoops @ 320mm spacing; (c) specimens with steel spirals @ 75mm pitch; (d) comparison between specimens confined with CFRP and GFRP; (e) GFRP confined specimens with or without fibers oriented in the longitudinal direction; (f) CFRP confined specimens with or without fibers oriented in the longitudinal direction;

***Confinement by FRP shells vs. confinement by lateral steel:*** The objective of the following comparisons is to evaluate the potential of FRP shells in replacing the conventional steel as lateral reinforcement. A comparison can be made between specimens 3 or 4, with only confinement from hoops at 320mm, and specimen 9, shelled with one layer of GFRP. As can be observed from Table 1, the total load carrying capacity, ductility factor, energy capacity, and work index of specimen 9 are all significantly higher than those of specimens 3 or 4. Some parameters of specimen 9, such as ductility factor and work index, are competitive with those of specimens with confinement from #3 spirals at 75mm pitch. These reveal that a layer of GFRP applied can safely replace the US#3 hoops at 320mm from confinement effectiveness point of view. Similarly, by comparing specimen 11 with specimens 5 or 6, it is obvious that a shell containing 2 layers of GFRP is superior to US #3 spirals at 75mm pitch. Similar conclusion can be drawn by comparing specimen 20, having one layer of CFRP, with specimens 5 or 6. Therefore, columns of the size tested here with one layer of CFRP or two layers of GFRP demonstrate better performance than those designed for seismic resistance with US#3 spirals at 75mm pitch.

***Confinement by CFRP shell vs. confinement by GFRP shell:*** For equal number of layers of FRP, CFRP shell is found to be more efficient than GFRP in improving the performance of columns. To evaluate this, a comparison can be made between the following three sets of specimens: 7 and 20, 11 and 24, 15 and 24 (Fig. 3d and Table 1). The specimens in the first two pairs of specimens contained no lateral steel, with the specimens in the first pair confined with one layer of GFRP and CFRP. Each specimen in the second pair (# 11 and 24) contained two FRP layers. By comparing the strength enhancement, ductility factor, and energy absorption capacity, it is obvious that specimen with one layer of CFRP exhibited better column performance than that of column with one layer of GFRP. Similarly, specimen with two layers of CFRP was much superior in performance to specimen containing two layers of GFRP. Column 15 contained #3 spirals at 75mm pitch in addition to 2 layers of GFRP while specimen 24 contained only 2 layers of CFRP. Comparison of specimen 15 with 24 indicates that strength and ductility improved by two layers of CFRP exceeded what was gained from two layers of GFRP and spirals at 75mm pitch as well. Specimen 24 demonstrated higher ductility factor and energy absorption capacity $e_{80}$ than specimen 15 but the energy absorption capacities $e_{50}$ and $e_{20}$ were comparatively. This implies that the degradation of confined concrete at large strains is more rapid in specimen 24, or in other word, specimen 15 exhibited more ductile post-peak behavior (Fig. 3d). The difference in the degradation of confined concrete can be attributed to the fact that two confining materials, both GFRP and lateral steel, for specimen 15 can sustain higher strain in the hoop direction than CFRP in specimen 24.

***Effect of longitudinal fibers on column behavior:*** Four pairs of specimens are compared to investigate the effect of longitudinal fibers: specimens 7 and 8, specimens 11 and 12, specimens 20 and 19, and specimens 24 and 25 (Figs. 3e and 3f). All these specimens contained no lateral steel. In each pair, the second specimen is different from the first due to the presence of FRP with fibers in the longitudinal direction. It can be found from first three pairs (Table 1) that 1 or 2 layers of GFRP or 1 layer of CFRP in the longitudinal direction considerably improved the strength of confined concrete column while the contribution toward improving the ductility parameters was minimal. No strength enhancement was observed by adding two layers of CFRP in the longitudinal direction (Fig. 3f). Thus, it is inconclusive regarding the strength enhancement by adding CFRP layers with fiber oriented in the longitudinal direction. However, one phenomenon was observed steadily by adding FRP in the longitudinal direction. As shown in Figs. 3e and 3f, specimens with longitudinal CFRP or GFRP were found to have the first ascending branch of the stress-strain curve extended to a higher stress than those lacking of longitudinal FRP. This phenomenon may be due to the stiffness increase of FRP shells. The fibers in the longitudinal direction are not likely to increase the stiffness of the shell in the lateral direction. However, increase in the amount of epoxy, introduced by adding the longitudinal fibers, would improve the stiffness of FRP shell as a whole. The stiffer jacket may have delayed the occurrence of second branch by delaying the propagation of concrete cracks.

***Size effect:*** An extensive literature search that most of the experimental work on FRP confined concrete was carried out on small-scale specimens. Almost all the small-scale FRP-confined specimens exhibited bilinear response without post-peak response, while most of the large size columns displayed descending branch of response under concentric compression (Kestner et al. 1997, Demers and Neale 1999). Large scale specimens are compared with the small-size cylinders, 152mm in diameter and 305mm in length, to investigate the size effect on the FRP confined concrete. For the cylinder tests, three concrete strengths ranging from 46MPa to 112MPa were utilized and four different types of FRP jackets were applied. No steel reinforcement was used in the cylinders. In this study, a select group of cylinders wrapped with the same two types of FRP composites as used in large scale columns discussed above, were considered. Table 2 presents details of cylinders along with those of the comparable large column specimens. Results for the cylinder tests shown in the table represent the average values for two specimens.

Table 2. Comparison between small- and large- scale specimens.

| Spec. Name | diameter (mm) | FRP layers | $f_{co}$ * (Mpa) | $\varepsilon_{co}^{\#}$ | $f_{ccmax}$ (Mpa) | $\varepsilon_{cc}'$ | Conf. pressure $f_l$ (MPa) | k = $f_{ccmax}/f_{co}$ | $f_l/f_{co}$ | $\varepsilon_{cc}'/\varepsilon_{co}$ |
|---|---|---|---|---|---|---|---|---|---|---|
| G01-00-7 | 356 | 1GFRP | 29.8 | 0.0018 | 34.77 | 0.0037 | 3.01 | 1.167 | 0.101 | 2.06 |
| G02-00-11 | 356 | 2GFRP | 29.8 | 0.0018 | 44.82 | 0.0120 | 6.01 | 1.504 | 0.202 | 6.66 |
| C01-L0-20 | 356 | 1CFRP | 29.8 | 0.0018 | 43.9 | 0.0089 | 4.97 | 1.473 | 0.167 | 4.93 |
| C02-00-24 | 356 | 2CFRP | 29.8 | 0.0018 | 59.3 | 0.0138 | 9.94 | 1.990 | 0.334 | 7.64 |
| L2G1 | 152 | 1GFRP | 46.9 | 0.0022 | 59.1 | 0.0135 | 8.13 | 1.259 | 0.173 | 6.07 |
| L2G2 | 152 | 2GFRP | 46.9 | 0.0022 | 88.9 | 0.0221 | 16.26 | 1.896 | 0.347 | 9.96 |
| L1C1 | 152 | 1CFRP | 48.05 | 0.0022 | 80.9 | 0.0151 | 11.13 | 1.683 | 0.232 | 6.81 |
| L1C2 | 152 | 2CFRP | 48.05 | 0.0022 | 109.4 | 0.0201 | 22.27 | 2.276 | 0.463 | 9.06 |

* Unconfined concrete specimen strength
\# Strain corresponding to $f_{co}$

Two groups of specimens are compared to evaluate size effect on FRP confinement effectiveness: specimens L2G1 and L2G2 vs. specimens 7 and 11; and specimens L1C1 and L1C2 vs. specimens 20 and 24. L2G1 and L2G2 are cylinders with unconfined concrete strength of 46.9MPa and were wrapped with one and two layers of GFRP, respectively. They correspond to columns 7 and 11 that also contained one or two layers of GFRP. The second group is similar but the specimens are confined with CFRP. Due to the difference in unconfined concrete strength of specimens, stresses and strains of specimens were normalized with respect to the stress and strain of the corresponding unconfined concrete at peak stress, respectively (Figs. 4 and 5).

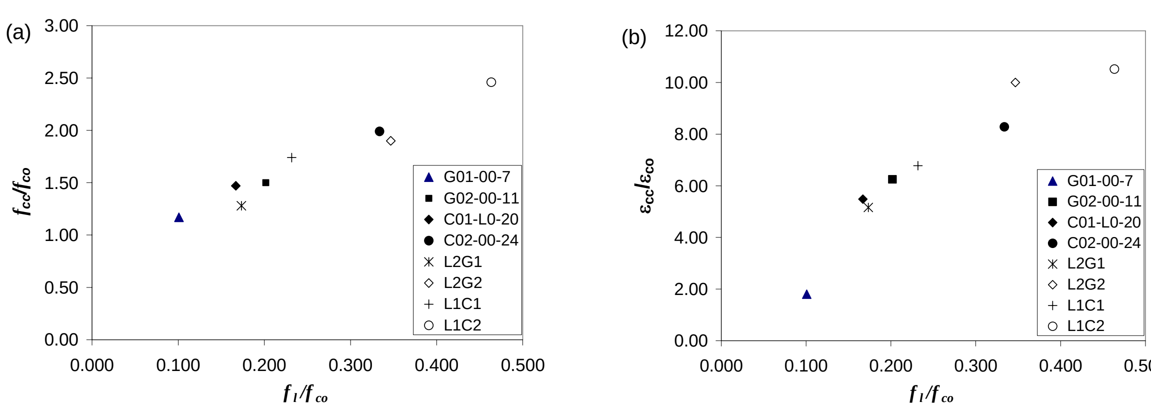


Figure 4. (a) strength enhancement vs. lateral confinement ratio (b) improvement in strain corresponding to peak stress vs. lateral confinement ratio.

Considering the lateral confining stress ratio ($f_l/f_{co}$), it can be observed from Table 2 that columns with two layers of GFRP/CFRP are comparable with cylinders with one layer of GFRP/CFRP. As demonstrated in Figs. 4a and 4b, specimens with similar confinement ratio gained similar improvement in confined concrete strength and the corresponding strain, regardless of the specimen size. The specimen size thus seems to have no any effect on the strength of the confined concrete and the corresponding strain.

However, by examining the stress-strain response of the concrete, the size of specimens visibly influenced the specimen performance. For instance, as can been seen from Table 2, cylinder L2G1 with one layer of GFRP obtained confinement ratio of 0.173 which is close to 0.202, the confinement ratio obtained by column G02-00-11 with two layer of GFRP. The similar lateral confinement ratio led to similar pre-peak response of the specimens but produced distinctly different post-peak response (Fig. 5a). Column G02-00-11 exhibited a slow degradation of the descending branch while cylinder L2G1 had the strength dropped dramatically. This phenomenon can be also observed for specimens confined with CFRP, demonstrating the ductile failure of large scale columns. The large area under stress strain curve of large-scale specimens due to ductile post-peak response indicates excellent energy absorption capacity of columns under axial load. It is worth noting that cylinder L1C2 confined with two layers of CFRP failed abruptly and only a couple of load steps and the corresponding deformations were recorded by the high speed data acquisition system before complete collapse of the specimen. This data was thus considered to lack reliability and was ignored.

The rupture mechanism of FRP at failure of specimens may explain the different failure mode due to specimen size. From the tests on columns, it was observed that FRP jackets normally unzipped along the longitudinal direction starting from a certain location in the test region and several FRP rings formed by the time specimen lost most of its loading capacity. In contrast, no unzipping process in the small cylinders was observed before sudden collapse of specimens. This phenomenon is reasonable since, for large scale columns, a substantial length of FRP needs to rupture before the column completely loses its load carrying capacity. While for small size specimens, only a small length of FRP needs to rupture before the specimen suddenly loses its strength. Thus gradual unzipping of FRP jackets in large scale columns results in the relatively ductile failure mode of column.

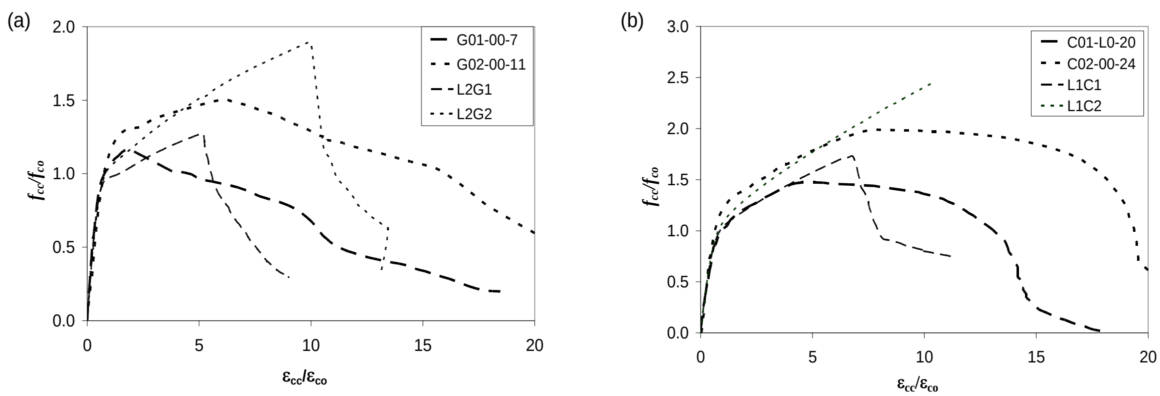


Figure 5. Comparison between normalized stress-strain curves of large-scale columns and small-scale cylinders: (a) GFRP confined specimens; (b) CFRP confined specimens.

## Conclusions

Columns with diameter of 356mm and height of 1524mm were tested in the present study. The experimental results show that the FRP shells can be successfully used as stay-in-place formwork while providing effective confinement reinforcement for concrete columns. FRP shells can efficiently substitute for the lateral reinforcement and avoid congestion that may result in lower quality concreting and increased cost of construction.

Following conclusions can be drawn from the results of this study:

1. There was a significant increase in compressive strength, axial strain at peak stress, ductility and energy absorption capacity of concrete columns owing to the confinement provided by FRP shells.

2. Glass fibers in the longitudinal direction enhanced the load carrying capacity of the columns but their contribution toward improving the ductility parameters was minimal. No definite conclusion could be made for the effect of carbon fibers in the longitudinal direction on the strength and ductility enhancement. However, for both CFRP and GFRP, fibers in the longitudinal direction extended first ascending branch linearly to a higher stress level prior to the softening of the column behavior.

3. From the strength and ductility points of view, FRP shells can effectively replace the lateral steel. The required number of FRP layers will depend on the amount of lateral steel that needs to be replaced.

4. CFRP shells, compared with GFRP shells, are more efficient in improving the performance of columns. Strength of the specimen with 2 layers of CFRP exceeded that of specimen confined with both 2 layers of GFRP and #3 spirals at 75mm pitch. The latter degraded in a slower manner after peak strength due to higher ultimate strains of GFRP and steel.

5. For the large scale columns and small cylinders tested for this investigation, no size effect on strength enhancement and ductility improvement was observed. However, it was demonstrated that larger columns failed in a more ductile fashion. Failure mechanism of FRP jacket observed from the test may explain the failure mode difference between columns and cylinders.

## Acknowledgments

Research work herein was supported by grants from Natural Sciences and Engineering Research Council (NSERC) of Canada and ISIS (Intelligent Sensing for Innovative Structures) Canada. Financial and technical contributions from Fyfe Company and R. J. Watson, Inc. are gratefully acknowledged. Experimental work was conducted at the Structures Laboratories of the Department of Civil Engineering at the University of Toronto.

## References

ASTM Standard A370-00. 2000. Standard test methods and definition for mechanical testing of steel products. Annual Book of ASTM Standards, Vol. 01.04.

ASTM Standard C39/C39M-00. 2000. Standard test method for compressive strength of cylindrical concrete specimens. Annual Book of ASTM Standards, Vol. 04.02.

ASTM Standard D3039-00. 2000. Standard test method for tensile properties of polymer matrix composite materials. Annual Book of ASTM Standards, Vol. 15.03.

Cairns, S. W. and S. A. Sheikh, 2001. Circular concrete columns externally reinforced with pre-fabricated carbon polymer shells. *Research Report No. SC-01-01*, University of Toronto, Toronto.

Demers, M. and K.W. Neale, 1999. Confinement of reinforced concrete columns with fiber-reinforced composite sheets-an experimental study, *Canadian Journal of Civil Engineering* 26, 226-241.

Jaffry, S.A.D. and S. A. Sheikh, 2001. Concrete filled glass fiber reinforced polymer (GFRP) shells under concentric compression. *Research Report No. SJ-01-01*, University of Toronto, Toronto.

Kestner, J.T., K. A. Harries, S. P. Pessiki, R. Sause and J. M. Ricles, 1997. Rehabilitation of reinforced concrete columns using fiber reinforced polymer composite jackets, ATLSS Report, Lehigh University, Bethlehem, PA.

Sheikh, S.A. and S. M. Uzumeri, 1980. Strength and ductility of tied concrete columns. *Journal of the Structural Division* 106 (5), 1079-1102.